ARGITU RFQ BEAD-PULL TUNING AND RF TESTS AT ESS-BILBAO

J. L. Muñoz*, I. Bustinduy, D. Fernández-Cañoto , N. Garmendia, P. González, G. Harper, J. Martín
ESS-Bilbao, Zamudio, Spain

Abstract

In this paper we describe the static tuning procedure of the ARGITU/HiCANS-platform RFQ at ESS-Bilbao. The machining and assembly of the RFQ were finished during 2025. The cavity is a 3.1-m-long, four-vane structure operating at 352.2 MHz. It will accelerate a 40 mA (designed up to 65 mA) proton beam from 45 keV to 3.0 MeV. The RFQ will operate at 1 % duty cycle in the first stages of the ARGITU HICANS platform, and later as the injector of the linac at a maximum duty cycle of 5 %. The static tuning of the cavity has been carried out combining bead-pull field-profile measurements with a conventional SVD algorithm and a genetic algorithm, the latter required by the limited tuner range available near the operational frequency. The whole procedure and the results are described in this paper.

INTRODUCTION

The ARGITU RFQ is the first accelerating cavity of the ESS-Bilbao proton linac for the HiCANS platform project of a compact accelerator-driven neutron-source [1–3]. It is a 352.2 MHz, four-vane RFQ designed to accelerate protons from 45 keV to 3.0 MeV in a 3.1 m long copper structure [4–7]. One of the characteristics of ESS-Bilbao RFQ is that no brazing was used for the assembly of the vanes that form each segment.

The RFQ was assembled, and its alignment was verified by using mechanical probes and laser-tracker measurements. The RFQ is designed assuming a uniform inter-vane voltage of 85 kV, so in the ideal assembly the field profile along the RFQ length will be flat, as well as symmetric in the four lobes. The deviations from this ideal behavior are caused by the modulation itself as well as by perturbations caused by the assembly and mechanical deformations of the structure. As a result, the measured field in the four lobes is not flat along the longitudinal coordinate and is not identical in all quadrants. Tuning is therefore required to recover the design longitudinal field profile and to bring the resonant frequency close to the value that will be used in operation.

The RFQ has 64 tuner ports, two of which are occupied by the power-coupler ports in the final configuration. The tuning campaign was carried out with 62 plunger tuners installed. Each plunger tuner is attached to a high-precision manual actuator, with a total tuner range of 25 mm. The RFQ was placed in a laboratory room with controlled temperature, with the bead-pull apparatus attached. Figure 1 shows the RFQ installed in the bead-pull bench.

* jlmunoz@essbilbao.org

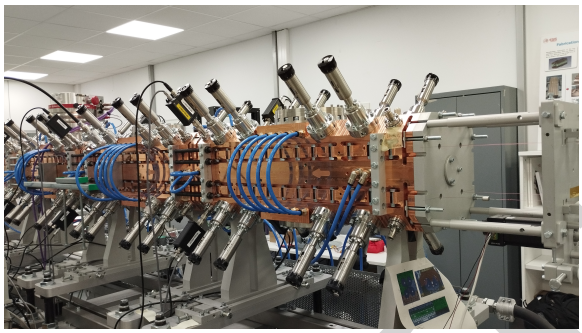

Figure 1: ESS-Bilbao RFQ installed in the bead-pull bench. The tuner actuators, pickup loops and bead-pull apparatus are visible.

BEAD-PULL MEASUREMENTS

The field profile was measured with the bead-pull technique. A small metallic bead was moved through high-magnetic-field lobe regions by the action of a computer controlled motor. The phase perturbation of the transmitted RF signal was recorded with a network analyzer. The bead moves along two of the lobes in the positive direction (beam direction), and along the negative one in the other two, so the data processing software needed to take care of this. The four traces were synchronized in the longitudinal direction using the perturbation caused by the first of the plunger tuners in the measured trace. Traces were then shifted to match this position. Finally, the base-line magnitude of the traces, in positions outside of the RFQ (which should be of zero amplitude) were used for height and drift compensation. The four longitudinal traces, $q_1(z)$ to $q_4(z)$, were assigned signs according to the quadrupolar-mode convention and normalized before being combined into the quantities $Q = \frac{q_1 - q_2 + q_3 - q_4}{4}$, $D_s = \frac{q_1 - q_3}{2}$ and $D_t = \frac{q_2 - q_4}{2}$.

The quadrupolar component Q represents the useful accelerating-field profile and is normalized to an average value of 100 %. The dipolar terms D_s and D_t quantify asymmetries between opposite lobes. The ideal tuning target used in the procedure is therefore a flat $Q(z)$ profile and dipolar components as close as possible to zero.

The initial configuration used for the response characterization had all tuners inserted to the same penetration. The measured profiles, shown in Fig. 2, presented a strong longitudinal slope in Q and large dipolar components. Nineteen longitudinal positions were selected from the traces to form the profile vector used by the tuning algorithms. The selected positions avoided regions where the bead passed too close to tuners, pickups or coupler openings, because such regions can create local distortions that are not representative of the global accelerating profile. Cavity frequency for this configuration was 349.995 MHz.

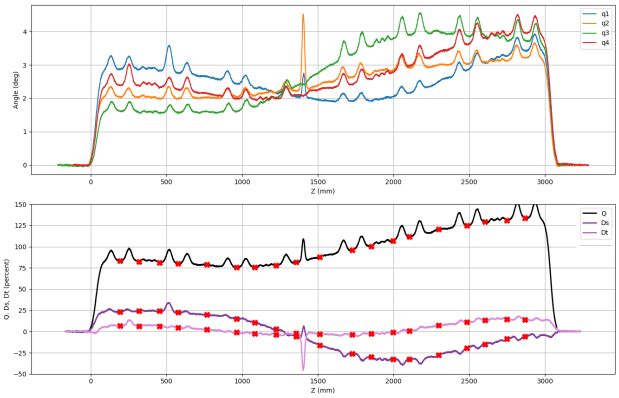

Figure 2: Initial bead-pull profiles for uniform tuner penetration. The quadrupolar component has a strong longitudinal slope and the dipolar components are large.

RESPONSE-MATRIX AND SVD TUNING

A response matrix of the tuners action on the field profiles was first constructed experimentally. Starting from a reference tuner configuration, each tuner was moved by a known amount and a complete bead-pull measurement was repeated. The resulting changes in Q, D_s and D_t at the selected (19) longitudinal positions define one column of the matrix M, of length 57-elements. In the small-perturbation approximation,

$$\Delta V = M \Delta T, \tag{1}$$

where ΔV contains the changes in Q, D_s and D_t, and ΔT is the vector of tuner-position changes. The response matrix M is then a 57×62 matrix. A visual representation of M is shown in Fig. 3.

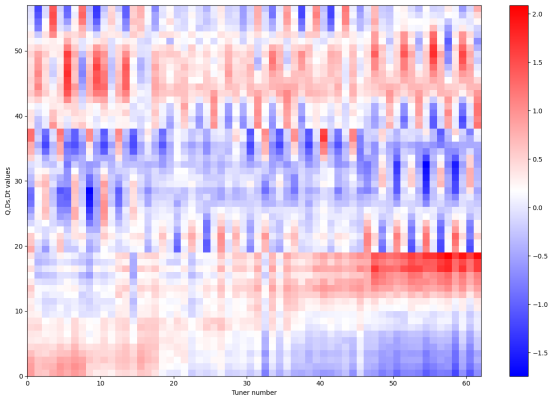

Figure 3: A color map representation of the response matrix M of the RFQ, relating the changes in tuner penetration to changes in the profile of Q, D_s and D_t profiles.

The conventional SVD approach [8–11] to get the optimal set of tuner penetration changes that would produce the right change in the field profiles to obtain the desired ones, involves an inversion of M matrix, such that the required change in tuners would be: $\Delta T = M^{-1}\,\Delta V$. As matrix M is not a square one, a pseudo-inverse computed from the SVD algorithm is used. This procedure identifies a set of optimal tuner changes. The best possible solution involves large changes in the tuners, although in an iterative approach it is possible to select proposed solutions with lower average tuner change but poorer performances.

The application of the SVD approach to the ESS-Bilbao was successful for the first steps of the tuning procedure. After three iterations, a field profile as the one shown in Fig. 4 was achieved. Field flatness as well as symmetry among the vanes was well achieved. This is shown in the uniformity of the Q profiles and in the very small magnitude of the D_s and D_t profiles.

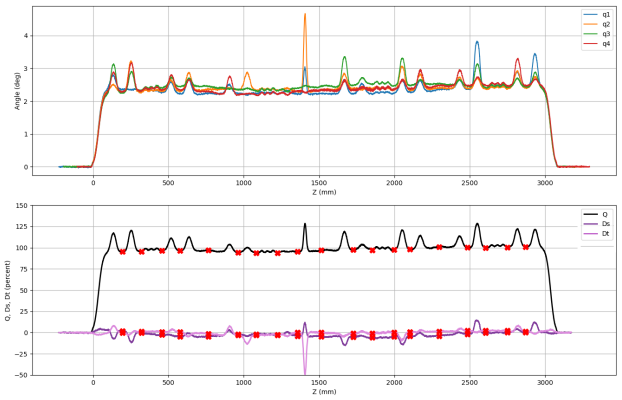

Figure 4: Field profiles after several iterations of the SVD algorithm. The field profiles are quite flat and with the asymmetries well compensated. Cavity frequency in this configuration was 350.192 MHz, not increased from the initial situation.

From this configuration, tuners were inserted uniformly to increase cavity frequency to the operational one. This required new bead-pull measurements and tuning runs, because the tuner penetration altered the field profiles equilibrium. With higher frequencies, that required larger tuner penetration in average, the application of the SVD algorithm was not possible in our case to continue the tuning procedure: the proposed tuner configurations involved tuner changes that were not physically possible due to the actuators moving range. Furthermore, increased tuner penetrations resulted in stronger perturbations of the measured profiles. To overcome these difficulties, an optimization approach based on a genetic algorithm has been successfully used.

GENETIC OPTIMIZATION

A constrained genetic optimizer was then used as an extension of the measured response-matrix approach. Each individual in the population represented a 62-component vector of tuner displacements. The measured matrix M was used as a forward model to predict the resulting profile, and the fitness was computed from the rms error of the predicted Q, D_s and D_t values with respect to the target profile. Hard penalties were applied when any tuner exceeded its mechanical limits, while softer penalties discouraged solutions too close to the boundaries.

The important practical advantage is that the optimizer solves the reachable problem rather than the unconstrained

inverse problem. As a result of the constraints in the available tuner ranges, a configuration that can actually be implemented on the RFQ is found. After each genetic-optimization step, the selected tuner configuration was set on the cavity, a new bead-pull measurement was performed, and the measured result became the next starting point. In between steps of application of the genetic algorithm tuning, cavity frequency was modified to approach the operating one. To reach this frequency target, strong tuner penetrations had to be set up, resulting in perturbations on the field profile. Each step a new measurement and a new run of the genetic algorithm was required. The procedure ended satisfactorily after several steps. The final tuning for the RFQ is shown in Fig. 5. In Fig. 6, the evolution of the tuning procedure is shown until final configuration is obtained.

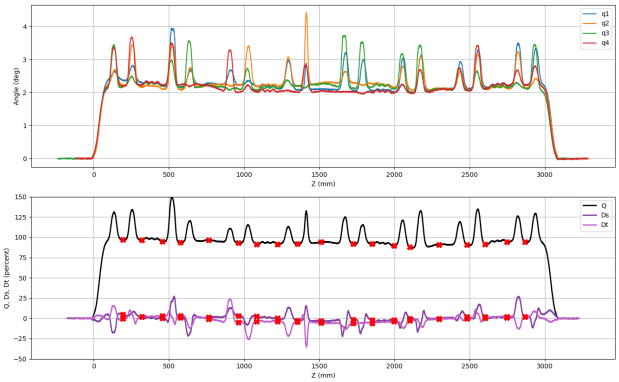

Figure 5: Field profiles after several iterations of the genetic algorithm. The field profiles are quite flat and with the asymmetries well compensated. Cavity frequency in this configuration was 352.100 MHz, the target frequency of the tuning procedure.

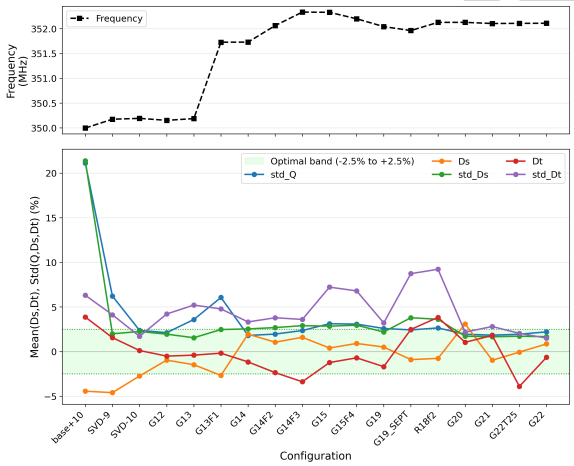

Figure 6: Evolution of the RFQ tuning procedure. Top: resonant frequency. Bottom: standard deviation of Q, D_s and D_t, and average values of D_s and D_t.

The method was previously tested with simulation studies [12] and was then applied to the real RFQ during the final tuning campaign. A more detailed description of the algorithm and the whole tuning procedure is described elsewhere [13].

REFERENCES

[1] M. Pérez, F. Sordo, I. Bustinduy, J. L. Muñoz, and F. J. Villacorta, "Argitu compact accelerator neutron source: a unique infrastructure fostering r&d ecosystem in euskadi", *Neutron News*, vol. 31, no. 2-4, pp. 19–25, 2020. doi:10.1080/10448632.2020.1819140

[2] J. Baggemann *et al.*, "High power target for the high brilliance neutron source", *Nucl. Instrum. Methods Phys. Res. A*, vol. 1069, p. 169912, 2024. doi:10.1016/j.nima.2024.169912

[3] Paulin, Mariano Andrés *et al.*, "The hermes reflectometer at the julic neutron platform", *EPJ Web Conf.*, vol. 286, p. 03003, 2023. doi:10.1051/epjconf/202328603003

[4] *ESS-Bilbao RFQ Technical Design Report DAES*, I. Bustinduy and J. L. Muñoz, Eds. Zamudio: ess-bilbao, 2015.

[5] J. L. Muñoz, I. Bustinduy, R. Igor, and D. de Cos, "Development of the radio frequency quadrupole proton linac for ess-bilbao", *EPJ Web Conf.*, vol. 231, no. 02001, pp. 173–196, 2020. doi:10.1051/epjconf/202023102001

[6] N. Garmendia *et al.*, "Status and RF Devopments of ESS Bilbao RFQ", in *Proc. LINAC'22*, Liverpool, UK, pp. 410–413, Oct. 2022. doi:10.18429/JACoW-LINAC2022-TUPOPA03

[7] J. Munoz *et al.*, "Update on ESS-Bilbao RFQ linac", in *Proc. LINAC'24*, Chicago, IL, USA, pp. 116–118, Aug. 2024. doi:10.18429/JACoW-LINAC2024-MOPB034

[8] T. P. Wangler, *Rf linear accelerators*. Weinheim: Wiley-VCH, 2008. doi:10.1002/9783527623426

[9] B. Koubek, A. Grudiev, and M. Timmins, "Rf measurements and tuning of the 750 mhz radio frequency quadrupole", *Phys. Rev. Accel. Beams*, vol. 20, no. 8, p. 080102, 2017. doi:10.1103/PhysRevAccelBeams.20.080102

[10] H. W. Pommerenke, U. van Rienen, and A. Grudiev, "Rf measurements and tuning of the 1-m-long 750 mhz radio-frequency quadrupole for artwork analysis", *Nucl. Instrum. Methods Phys. Res. A*, vol. 1011, p. 165564, 2021. doi:10.1016/j.nima.2021.165564

[11] W. Promdee, T. R. Edgecock, G. E. Boorman, J. K. Pozimski, and A. P. Letchford, "Bead Pull Measurements of the FETS RFQ at RAL", in *Proc. IPAC'17*, Copenhagen, Denmark, May 2017, pp. 4349–4351. doi:10.18429/JACoW-IPAC2017-THPIK108

[12] J. L. Muñoz *et al.*, "ESS-Bilbao RFQ Static Tuning Algorithm and Simulation", in *Proc. HB'23*, Geneva, Switzerland, pp. 440–442, Mar. 2024. doi:10.18429/JACoW-HB2023-THBP03

[13] JL. Muñoz and I. Bustinduy, "Frequency and field-profile tuning of the ess-bilbao rfq using a genetic optimization approach", *EPJ Res. Infrastruct.*, under review.